

# Supporting Information

## Ultra-Short Peptide Synthesis on Mesoporous Films and Its Impact on Ionic Mesopore Accessibility

Mohadeseh Bagherabadi<sup>a</sup>, and Annette Andrieu-Brunsen <sup>a\*</sup>

a. Department of Chemistry, Technical University of Darmstadt, Peter-Grünberg-Str. 4, 64287 Darmstadt, Germany.

\* [annette.andrieu-brunsen@tu-darmstadt.de](mailto:annette.andrieu-brunsen@tu-darmstadt.de)

## Characterization Section

### Characterization of BODIPY synthesis

BODIPY-COOH was synthesized as inspired by Williams et al. <sup>1</sup>. A red solid (130 mg, 37%) was obtained. <sup>1</sup>H NMR (300 MHz, CDCl<sub>3</sub>, δ): 1.04 (t, <sup>3</sup>J<sub>HH</sub> = 6.0 Hz, 6H), 1.98 (q, <sup>3</sup>J<sub>HH</sub> = 1.95 Hz, 2H), 2.34 (s, 3H), 2.40 (q, 4H), 2.50 (s, 3H), and 3.07 ppm (t, 2H); <sup>13</sup>C NMR (300 MHz, CDCl<sub>3</sub>, δ): 12.43, 13.31, 14.82, 17.19, 26.48, 33.99, 130.95, 132.84, 135.66, 143, 152.59, 178.19 ppm; MS (ESI): m/z calculated for C<sub>21</sub>H<sub>29</sub>BF<sub>2</sub>N<sub>2</sub>O<sub>2</sub> [M+H]<sup>+</sup> 391.2363; found 391.24 (Figure S1, S2, and S3a).

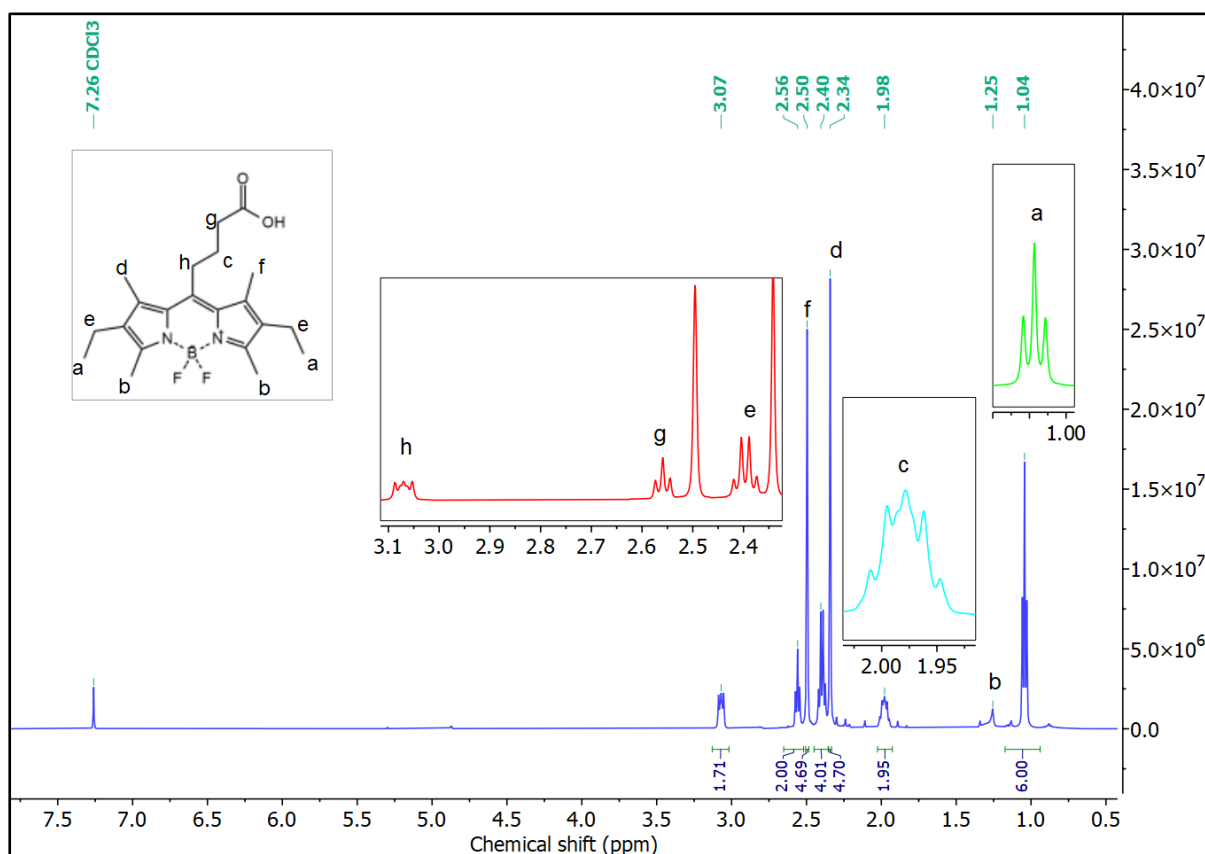


Figure S1. <sup>1</sup>H-NMR in CDCl<sub>3</sub> (300 MHz) from BODIPY-COOH.

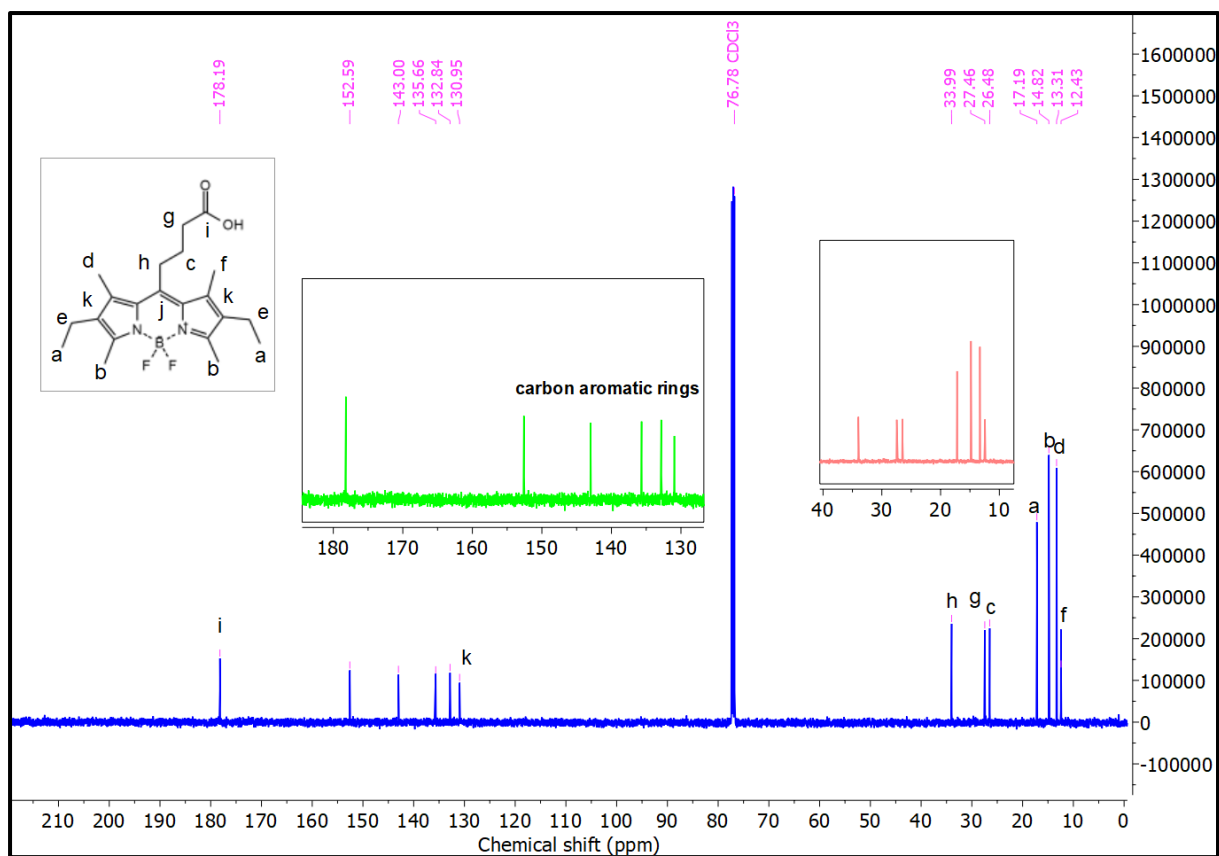
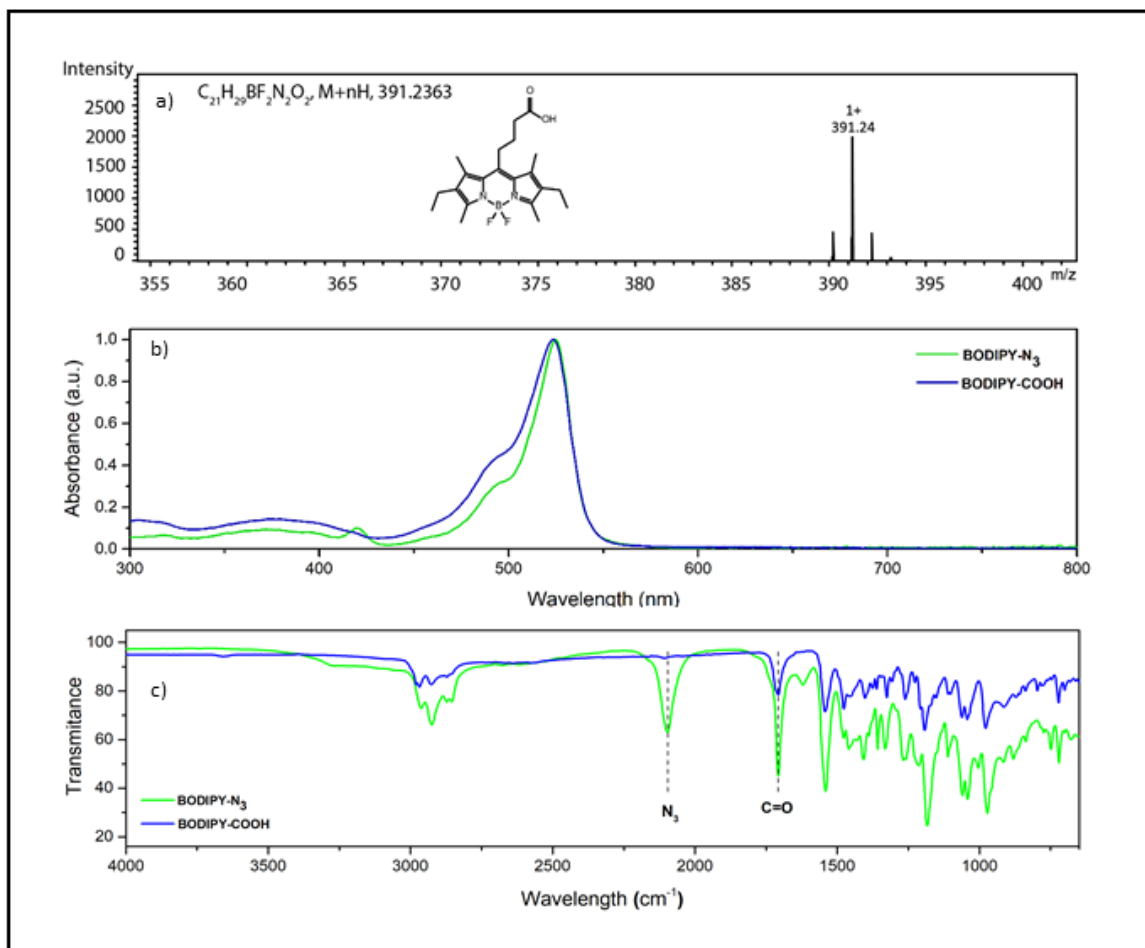


Figure S2. <sup>13</sup>C-NMR in CDCl<sub>3</sub> (300 MHz) from BODIPY-COOH.



**Figure S3.** a) ESI, b) normalized UV-VIs, c) ATR-IR spectra of synthesized dye (photocleavage-linker).

BODIPY-N<sub>3</sub> was synthesized as inspired by Strasser et al.<sup>2</sup>. This product was obtained as a red-orange solid (30 %). FT-IR spectra from BODIPY-COOH (Figure S3 blue) and after functionalization with the azide group show a N<sub>3</sub> vibration at 2200 cm<sup>-1</sup>, indicating that BODIPY-N<sub>3</sub> (Figure S3 green) was successfully synthesized (Figure S3c).

UV-Vis spectra were measured from BODIPY-COOH (Figure S3 blue) and BODIPY-N<sub>3</sub> (Figure S3 green) dissolved in DMF. UV-Vis spectra were recorded using Agilent Cary WinUV-Software.

Before each measurement, the background was automatically corrected. An absorption band can be observed in the UV spectral around 530 nm which is related to BODIPY (Figure S3b).

### ATR-IR from deprotected arginine and peptide-conjugation into the pore

ATR-IR spectrum of pure, deprotected arginine is shown in Figure S4. The vibrational band at  $1663\text{ cm}^{-1}$  and  $1091\text{ cm}^{-1}$  are attributed to the C=O stretching vibration of carboxyl group and C-N stretching vibration of amino acid, respectively<sup>3,4</sup>.

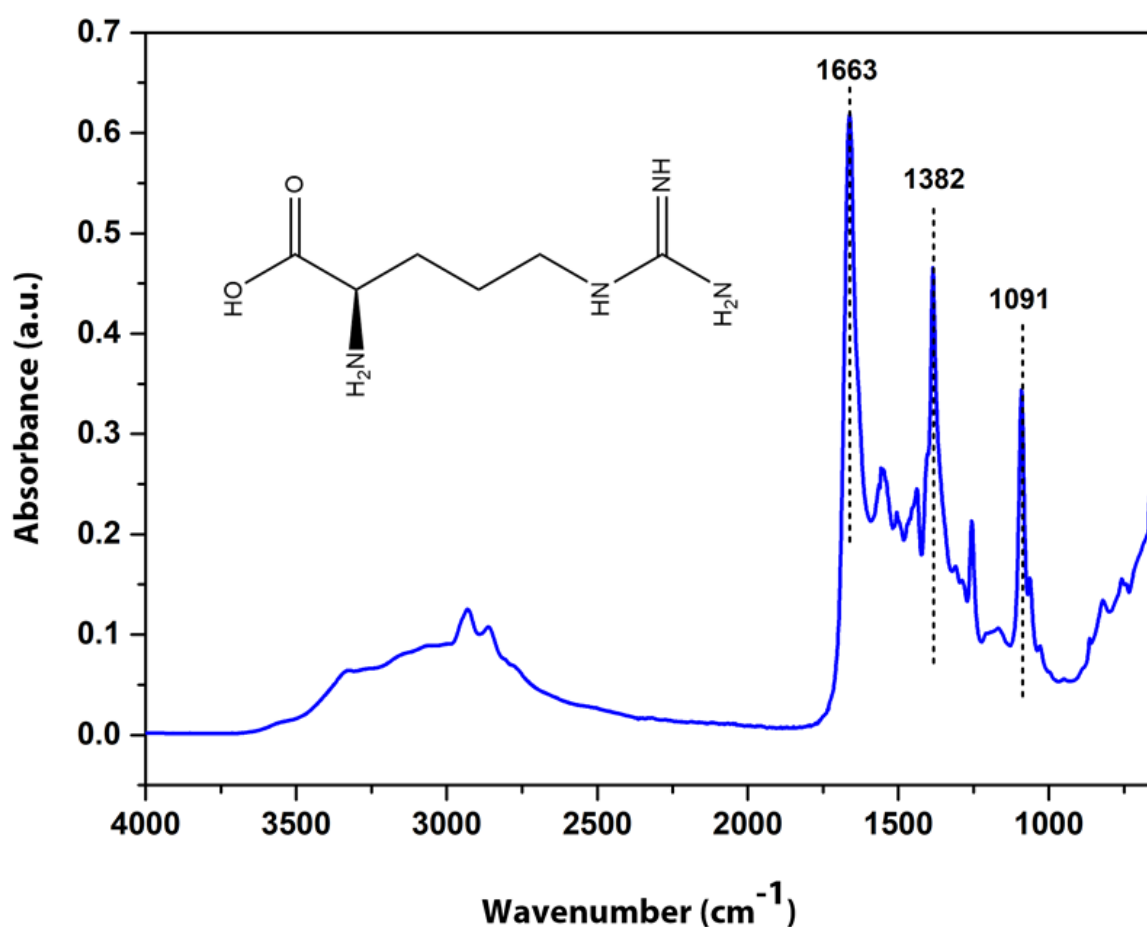
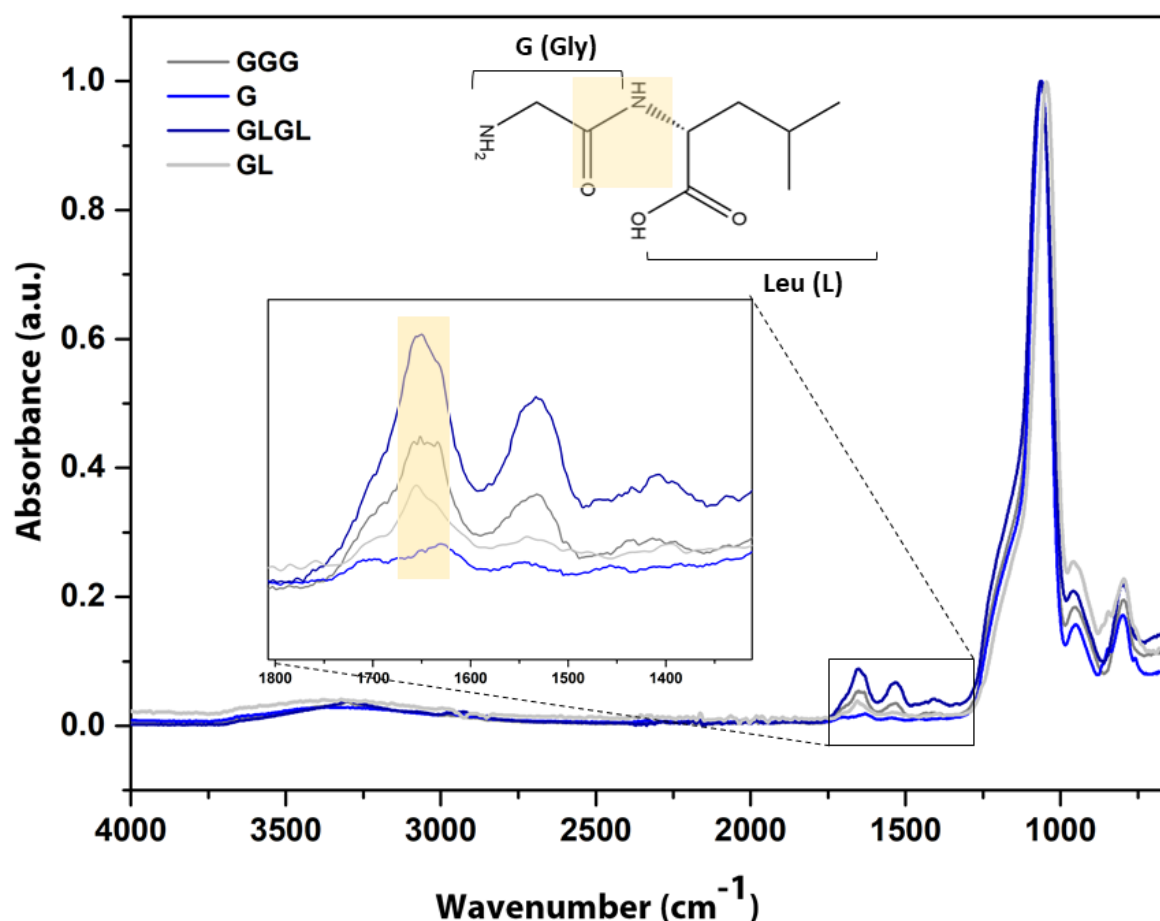


Figure S4. ATR-IR spectrum of deprotected arginine.

Various peptide sequences, including (GGG, GL, and GLGL), were synthesized and characterized for their presence in the mesoporous films using ATR-IR. Figure S5 displays the

ATR-IR spectra obtained from the films after the grafting of the peptide from the pore wall. The ATR-IR spectra show evidence of successful peptide grafting to the mesoporous films with different amino acids (Gly, Arg and Leu). The vibrational band at  $1660\text{ cm}^{-1}$  appears which is attributed to the peptide amide bond (amide I) in accordance with literature <sup>3,5-7</sup> (Figure S4). With increasing number of amino acid binding cycles, the stretching vibration of C=O at  $1660\text{ cm}^{-1}$  (amide I) in  $1080\text{ cm}^{-1}$  normalized ATR-IR spectra increased. Furthermore, a diagram of C=O stretching vibration at  $1660\text{ cm}^{-1}$  (amide I) versus adding different amino acids sequence is shown in Figure S6.



**Figure S5.** ATR-IR spectra of mesoporous silica film functionalized with Glycine, G (blue), GL (light grey), GLG (Gray), and GLGL (navy blue).

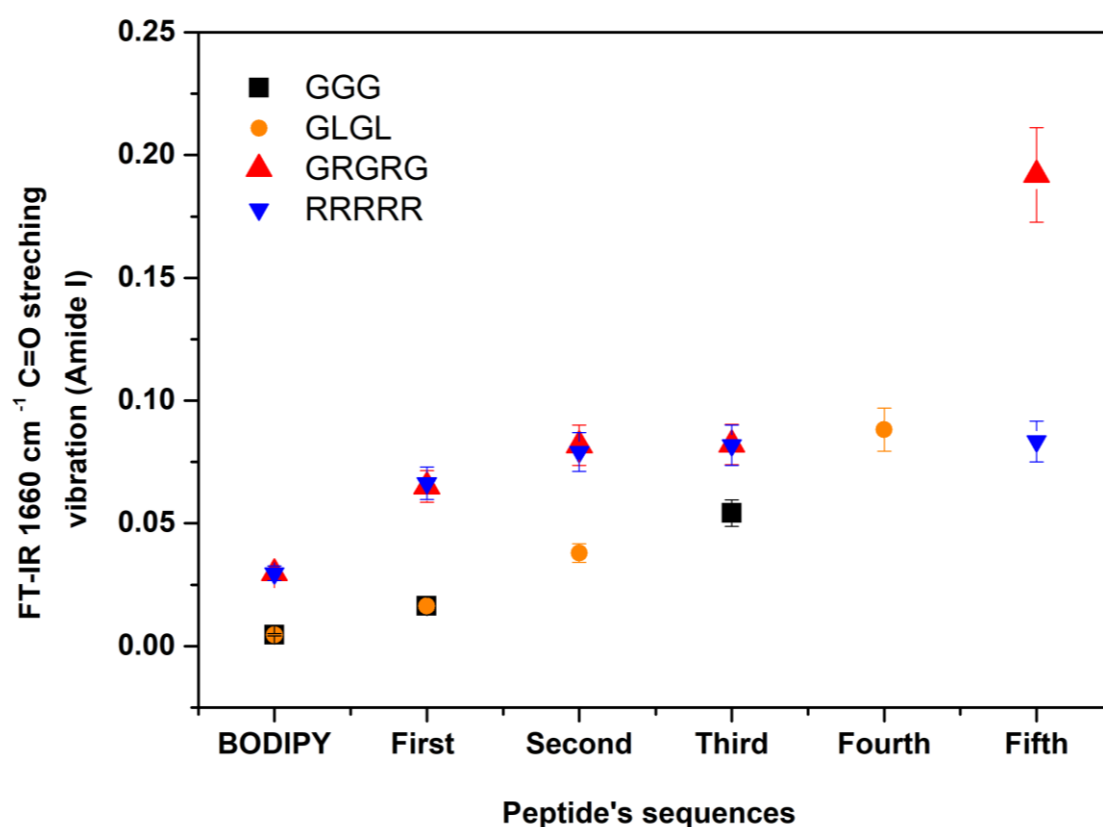


**Figure S6.** Diagram of stretching vibration of C=O at  $1660\text{ cm}^{-1}$  (amide I) versus adding amino acids sequences.

#### **ATR-IR from short peptide-mesoporous silica film with water as a reference**

To clearly identify the specific vibrational band associated with water and the peptide amide bond, the samples were prepared as follows: the film was carefully scratched from the glass substrate, and an ATR-IR analysis was conducted on the resulting sample (Figure S7, blue curve). Additionally, water (Figure S7, light blue) and deprotected arginine (Figure S7, navy) were separately added to the sample. ATR-IR spectra were then obtained from these samples.

The ATR-IR analysis revealed that the vibrational band observed at  $1660\text{ cm}^{-1}$  corresponds to the presence of the amide bond, indicating the successful grafting of the amino acid onto the film. Furthermore, the peak at around  $1625\text{ cm}^{-1}$  was identified as the characteristic vibrational band for water (Figure S8).

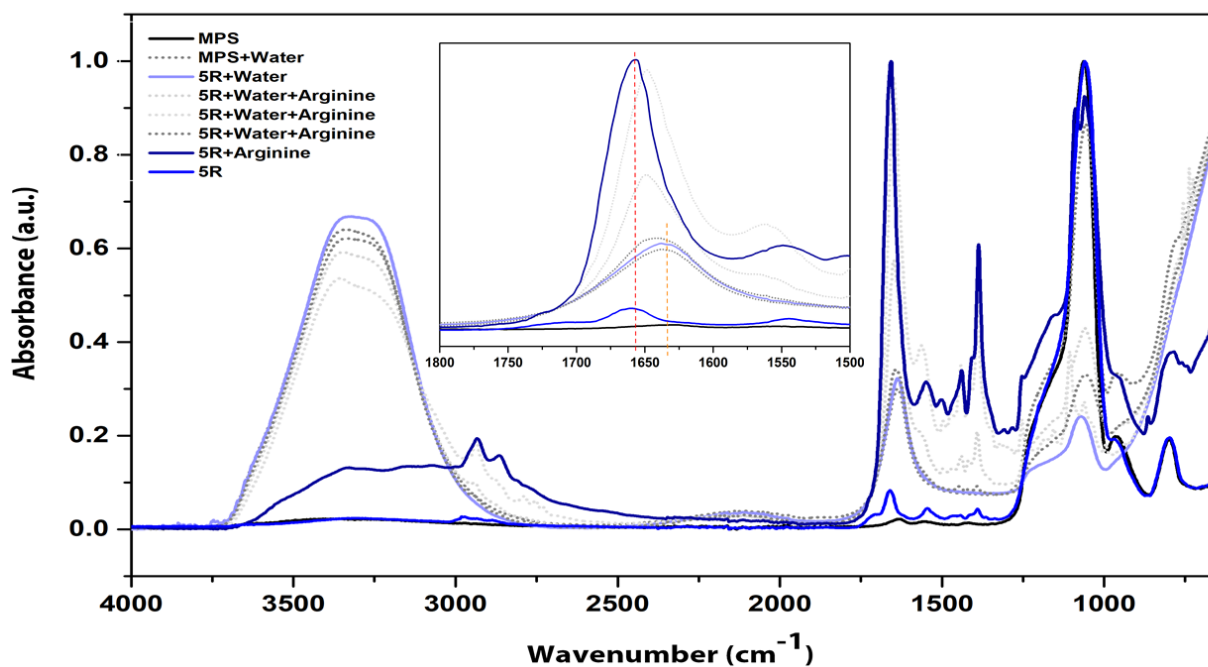


**Figure S7.** ATR-IR spectra of mesoporous silica film functionalized with 5R with exceeds arginine (Navy), 5R with water (light blue), and 5R (blue).

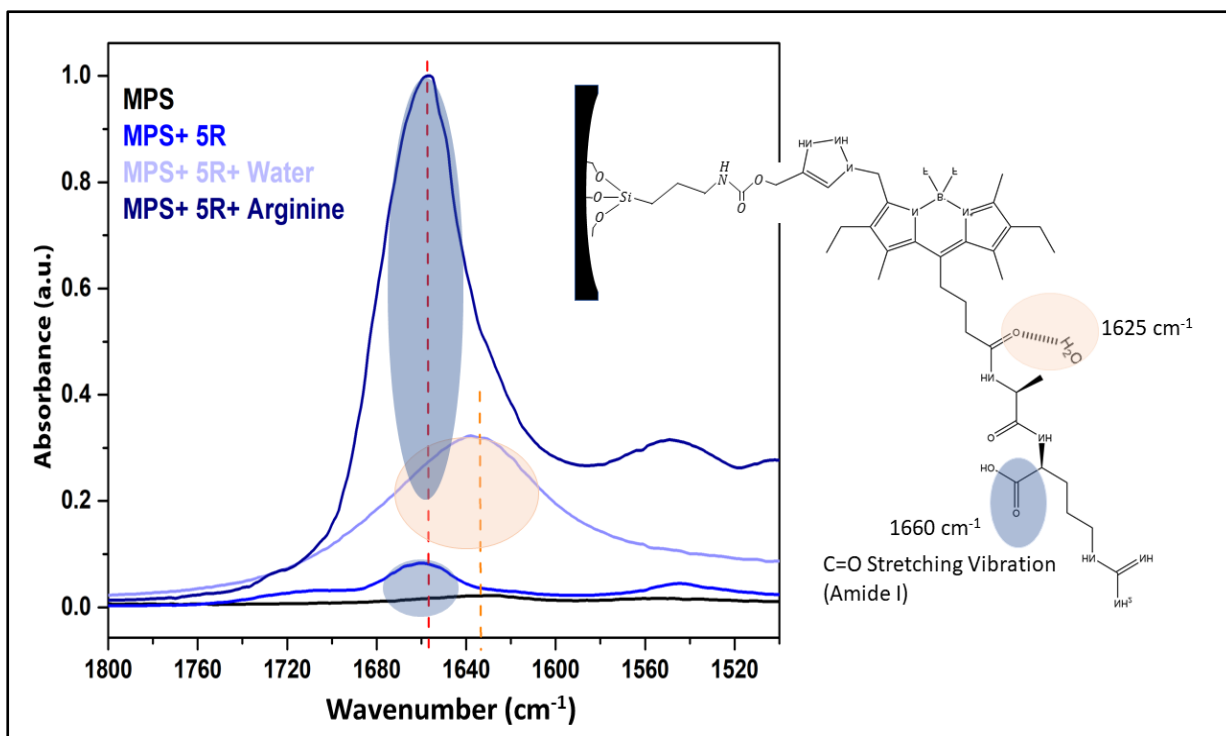


**Figure S8.** ATR-IR spectra of mesoporous silica film functionalized with 5R with exceeds arginine (Navy), 5R with water (light blue), and 5R (blue).

### Macroscopic static contact angle

The observation that the static contact angle (CA) of the grafting surface with PTEOS, BODIPY, and R up to 5R indicates that the surface of all these mesoporous films is relatively hydrophilic. It has to be noted that the macroscopic static contact angle of all samples remains between 58-38° (Figure S9). Thus, water is expected to imbibe into the mesoporous films.

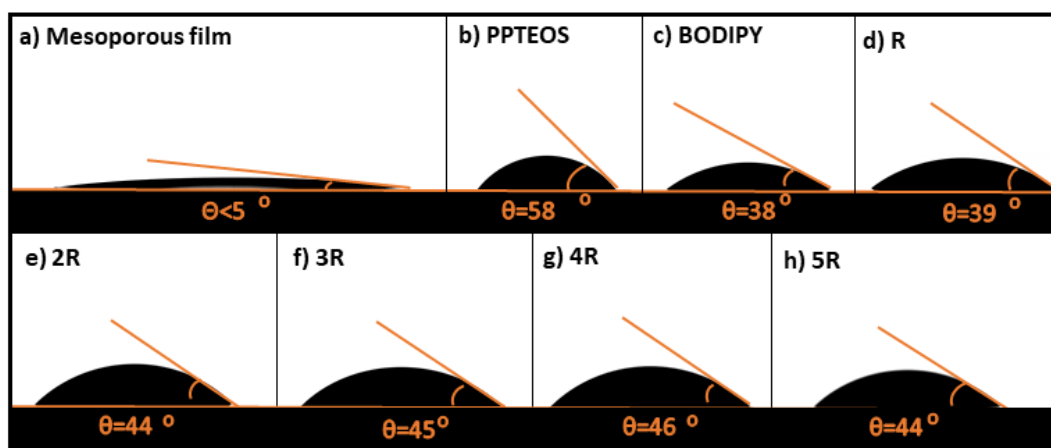


**Figure S9.** Static contact angles of a water droplet on the mesoporous film that functionalized with (a) non-functionalized; (b) PPTEOS; (c) BODIPY; (d) R; (e) 2R; (f) 3R; (g) 4R; and (h) 5R.

## Fluorescence properties

To analyze the fluorescence intensity of the samples that had been functionalized with BODIPY, 2R, and 5R grafting, the mesoporous silica films were scratched off their glass supports and dissolved in DMF as a solvent. The resulting solutions were then distributed over a wavelength range between 500 to 650 nm and excitation at 480 nm with a resolution of 1 nm, and their fluorescence spectra were measured (as shown in Figure S10). The spectral and fluorescent properties of the studied conjugates are primarily governed by the highest occupied molecular orbital (HOMO) - lowest unoccupied molecular orbital (LUMO) transition, with a significant contribution from the HOMO-1 - LUMO transition. The electron-donating amino acid moiety of the conjugate leads a higher HOMO energy level compared to the electron-withdrawing BODIPY component. Consequently, during photoexcitation of the conjugate, there is a favorable energy transfer from the amino acid moiety to the BODIPY moiety. This process, known as Photoinduced Electron Transfer (PeT), results in the quenching

of fluorescence in the conjugate <sup>8,9</sup>. As a result, a shift or change in fluorescence intensity occurs, indicating the successful conjugation process as visible in Figure S10.

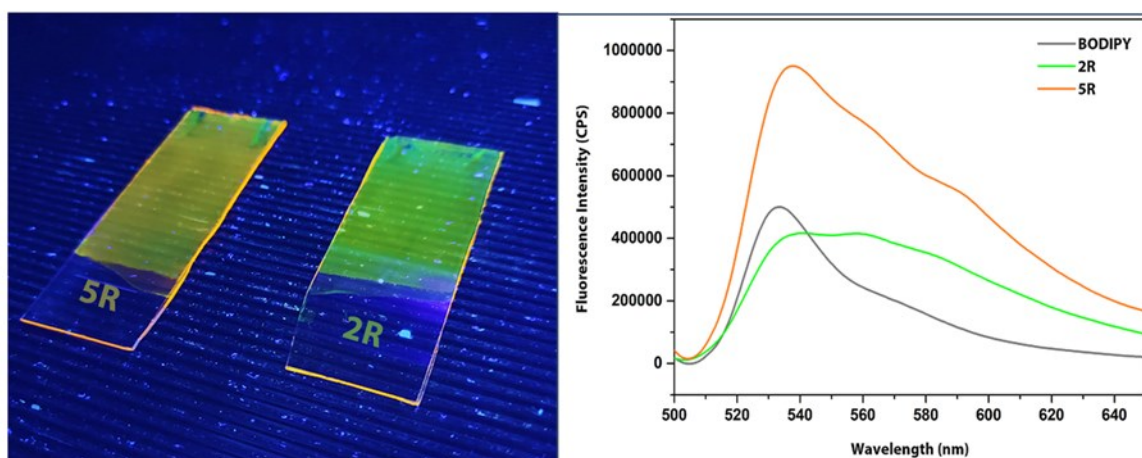


**Figure S10.** Right-Fluorescence spectrum of samples with BODIPY, 2R (green line), and 5R (orange line) conjugation of the surface. These spectra were obtained by exciting samples at 480 nm and emission was recorded from 510 to 650 nm. Left- Photo of samples with two and five sequences of arginine under a UV lamp.

## AUTHOR INFORMATION

### Corresponding Author:

**Annette Andrieu-Brunsen**, Department of Chemistry, Technical University of Darmstadt, Peter-Grünberg-Str. 4, 64287 Darmstadt, Germany. E-mail: [annette.andrieu-brunsen@tu-darmstadt.de](mailto:annette.andrieu-brunsen@tu-darmstadt.de), [Orcid.org/ 0000-0002-3850-3047](https://orcid.org/0000-0002-3850-3047)

### Author:

**Mohadeseh Bagherabadi**, Department of Chemistry, Technical University of Darmstadt, Peter-Grünberg-Str. 4, 64287 Darmstadt, Germany. [Orcid.org/ 0000-0001-9031-5281](https://orcid.org/0000-0001-9031-5281)

## References

1. Williams, T. M.; Zhou, Z.; Singh, S. S.; Sibrian-Vazquez, M.; Jois, S. D.; Henriques Vicente, M. d. G. J. P.; photobiology, Targeting EGFR Overexpression at the Surface of Colorectal Cancer Cells by Exploiting Amidated BODIPY-Peptide Conjugates. *J Photochemistry* **2020**, *96* (3), 581-595.
2. Strasser, P.; Russo, M.; Stadler, P.; Breiteneder, P.; Redhammer, G.; Himmelsbach, M.; Brüggemann, O.; Monkowius, U.; Klán, P.; Teasdale, I. J. P. C., Green-light photocleavable meso-methyl BODIPY building blocks for macromolecular chemistry. *J Polymer Chemistry* **2021**, *12* (47), 6927-6936.
3. Mudakavi, R. J.; Vanamali, S.; Chakravortty, D.; Raichur, A. M. J. R. a., Development of arginine based nanocarriers for targeting and treatment of intracellular Salmonella. *J RSC advances* **2017**, *7* (12), 7022-7032.
4. Raja, A. S.; Rajendran, S. J. J. o. E. S.; Engineering, Inhibition of corrosion of carbon steel in well water by arginine-Zn<sup>2+</sup> system. *J Journal of Electrochemical Science Engineering* **2012**, *2* (2), 91-104.
5. Zhu, J.; Han, H.; Li, F.; Wang, X.; Yu, J.; Qin, X.; Wu, D. J. C. o. M., Peptide-functionalized amino acid-derived pseudoprotein-based hydrogel with hemorrhage control and antibacterial activity for wound healing. *J Chemistry of Materials* **2019**, *31* (12), 4436-4450.
6. Lunn, J. D.; Shantz, D. F., Peptide Brush—Ordered Mesoporous Silica Nanocomposite Materials. *Chemistry of Materials* **2009**, *21* (15), 3638-3648.
7. Ruiz, D. S.; Cristobal, P. A.; Laurenti, M.; Retama, J. R.; Lopez-Cabarcos, E. In *Polymer Diffusion in Microgels with Upper Critical Solution Temperature as Studied by Incoherent Neutron Scattering*, Journal of Physics: Conference Series, IOP Publishing: 2014; p 012012.
8. Ksenofontova, K. V.; Ksenofontov, A. A.; Khodov, I. A.; Rummyantsev, E. V. J. J. o. M. L., Novel BODIPY-conjugated amino acids: Synthesis and spectral properties. *Journal of Molecular Liquids* **2019**, *283*, 695-703.
9. Ksenofontova, K. V.; Kerner, A. A.; Ksenofontov, A. A.; Shagurin, A. Y.; Bocharov, P. S.; Lukanov, M. M.; Kayumov, A. R.; Zhuravleva, D. E.; Iskhakova, Z. I.; Molchanov, E. E. J. M., Amine-Reactive BODIPY Dye: Spectral Properties and Application for Protein Labeling. *J Molecules* **2022**, *27* (22), 7911.